



T2K



KAVLI  
IPMU INSTITUTE FOR THE PHYSICS AND  
MATHEMATICS OF THE UNIVERSE

$\nu_{\mu}$  CC1 $\pi$  cross section on carbon and water  
using T2K on-axis detectors

Benjamin Quilain (Kavli IPMU, The University of Tokyo)

Matthieu Licciardi (LLR, Ecole polytechnique)

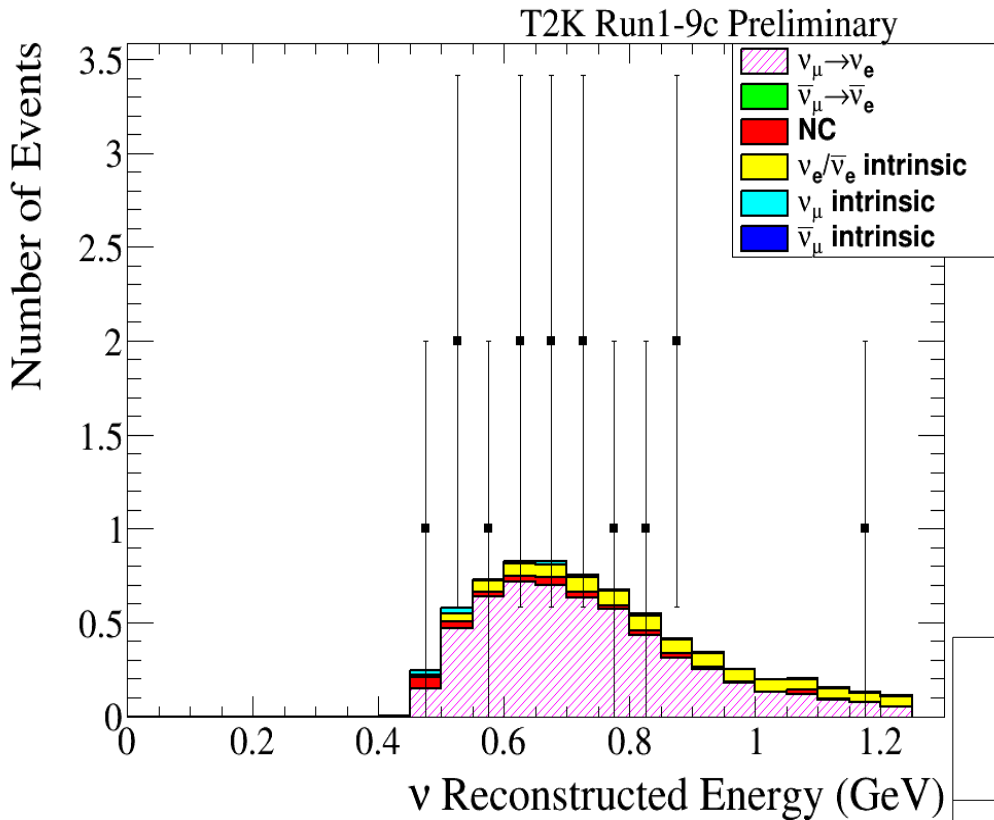
for the T2K collaboration

# Motivations

Use of CC1 $\pi$  channel to search for oscillation is increasing.  
 → T2K, Nova and future Hyper-K, DUNE

## T2K far detector

## But CC1 $\pi$ poorly known vs CC0 $\pi$ :



- Resonance model → RS ? Sobczyk ?  
Minoo ?
- Resonant mass value
- FSI models?

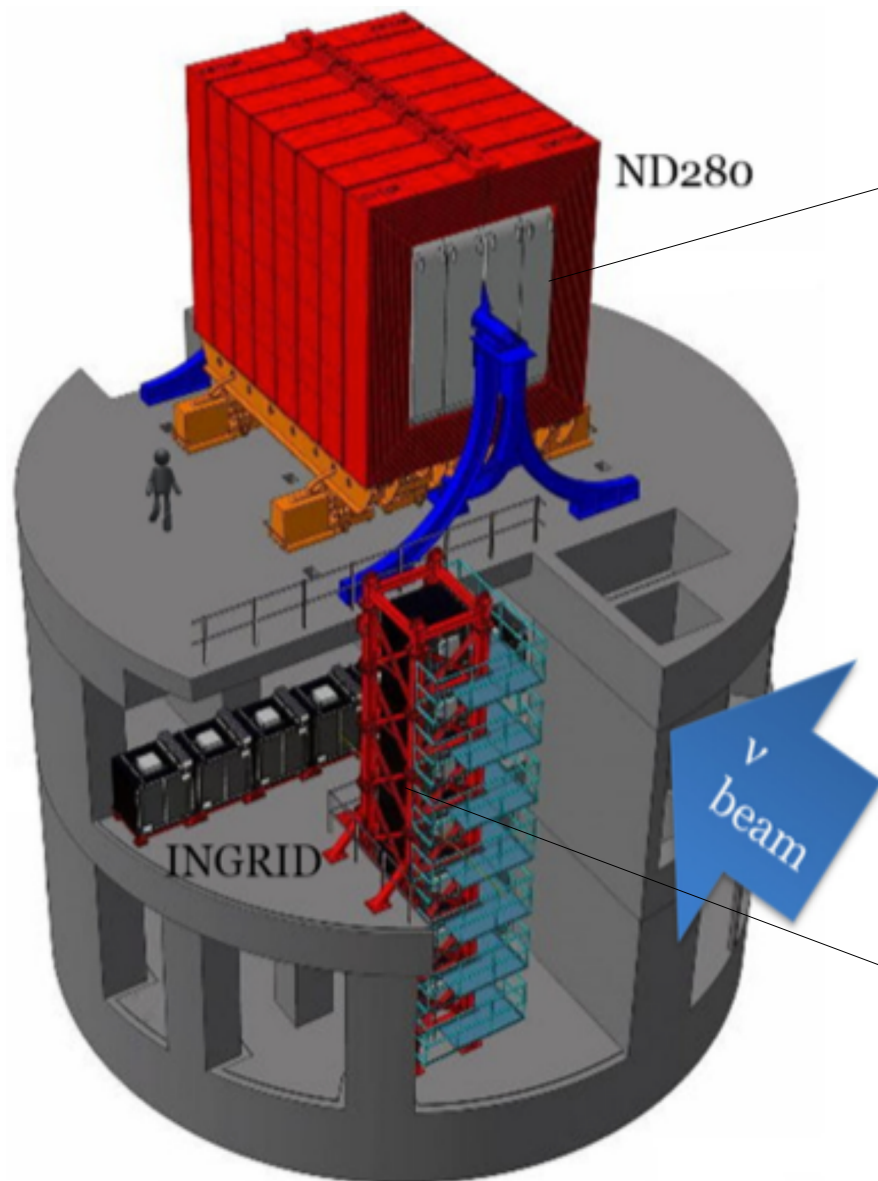
Main channel @T2K

	$\nu_{\mu}$ CCQE-like	$\nu_e$ CCQE-like	$\nu_e$ CC1 $\pi^+$ -like
Uncertainty	4.9 %	9.6 %	18.7 %

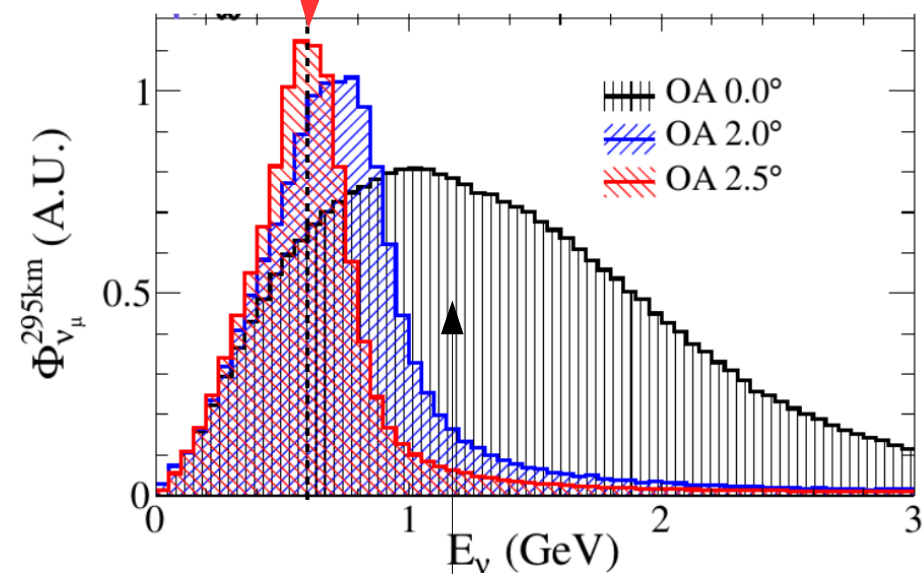
Goal : provide a more accurate CC1 $\pi$  measurement on H<sub>2</sub>O & CH

# T2K near detectors

Located at 280m from the target



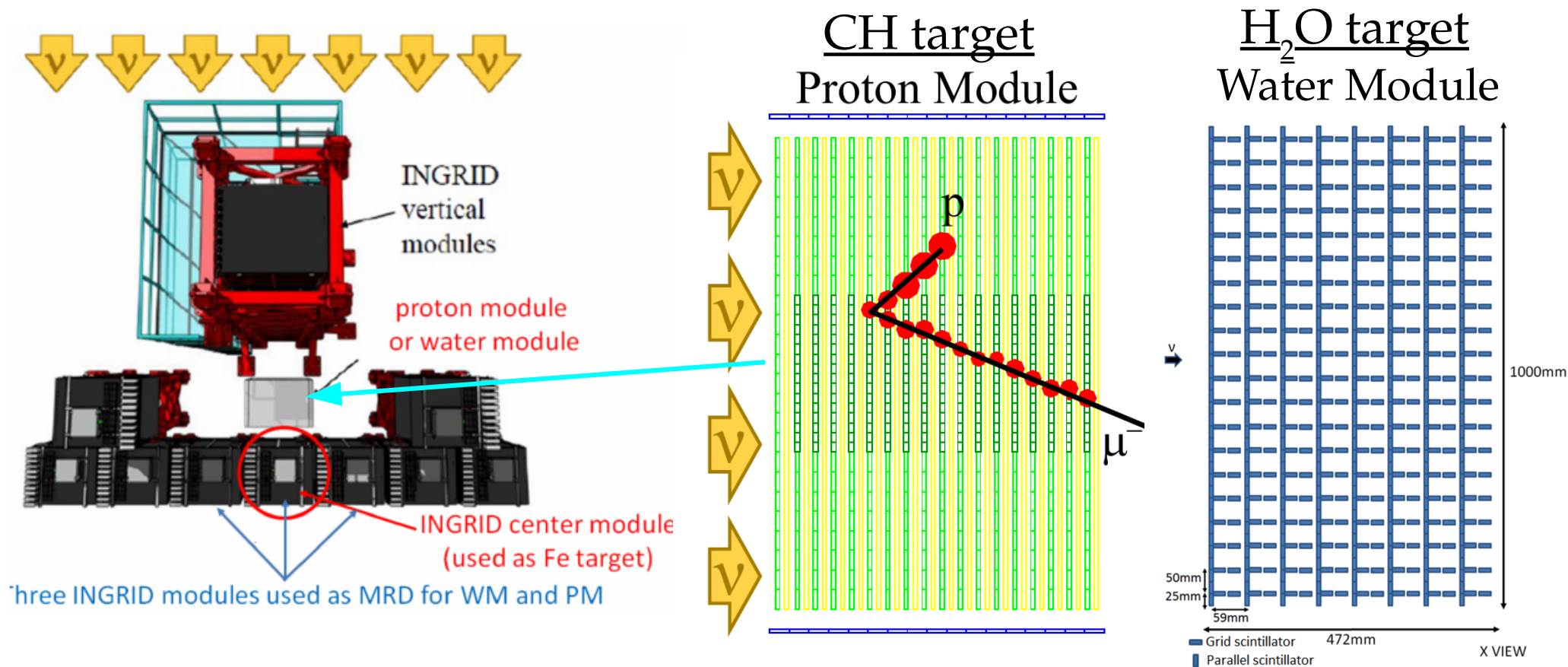
ND280 off-axis near detector



INGRID on-axis near detector

# Strategy to measure $CC1\pi$ cross-section

4



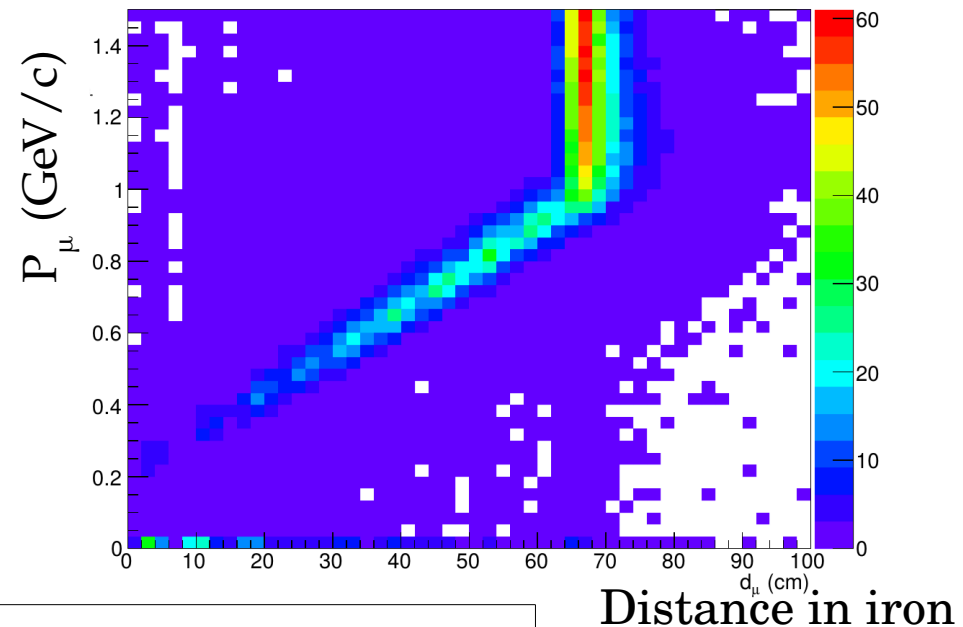
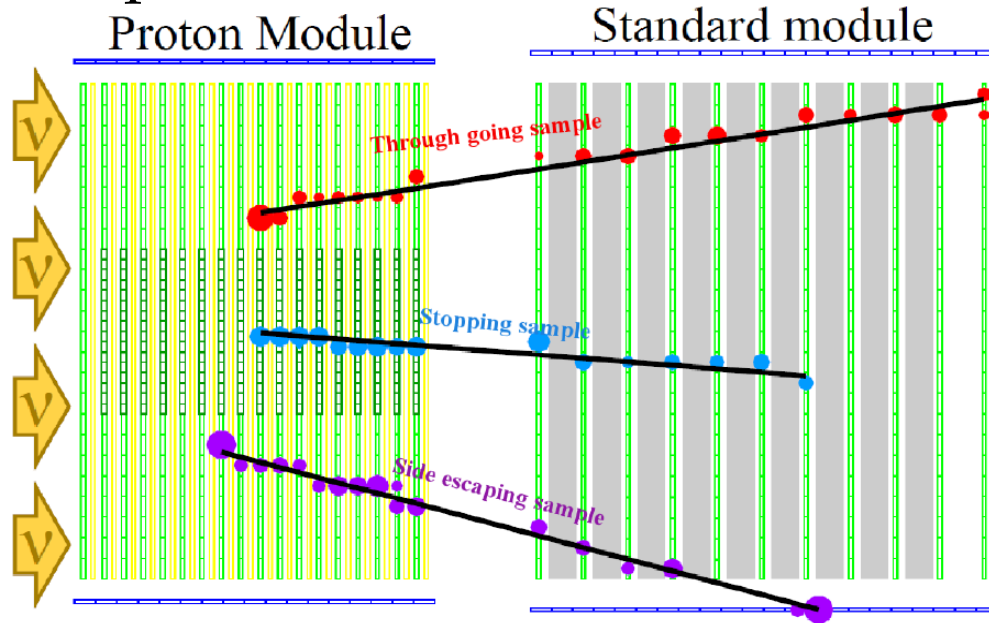
$H_2O$  and Plastic detectors installed at same position but different periods

- Proton Module (PM) :  $5.9 \times 10^{20}$  POT  $\nu$ -mode data in 2010 - 2013
- Water Module (WM) :  $7.2 \times 10^{20}$  POT  $\nu$ -mode data in 2016 – 2017

# Double differential cross section

- Aim to maximize model constraints  
 → Measurement differential in muon kinematics  $p_\mu, \theta_\mu$

- Use penetration distance of muon in iron to determine  $p_\mu$ .



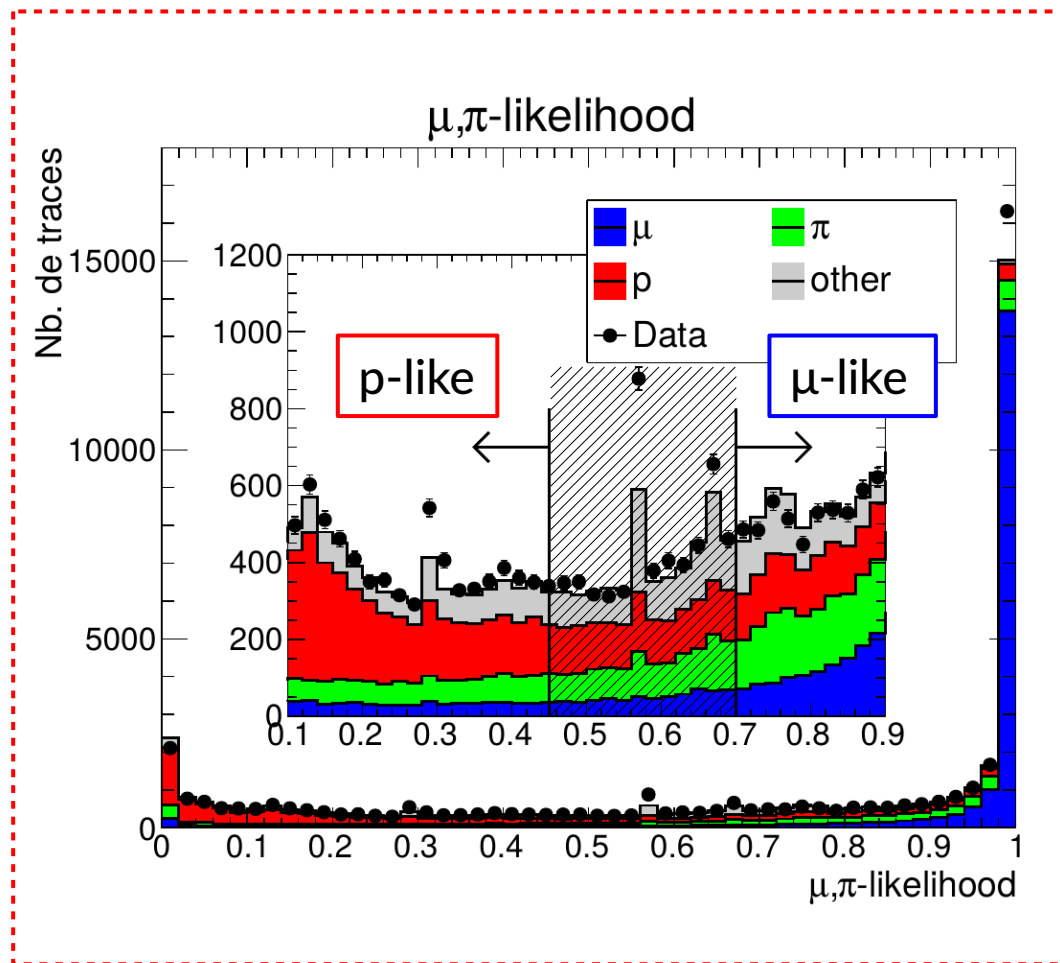
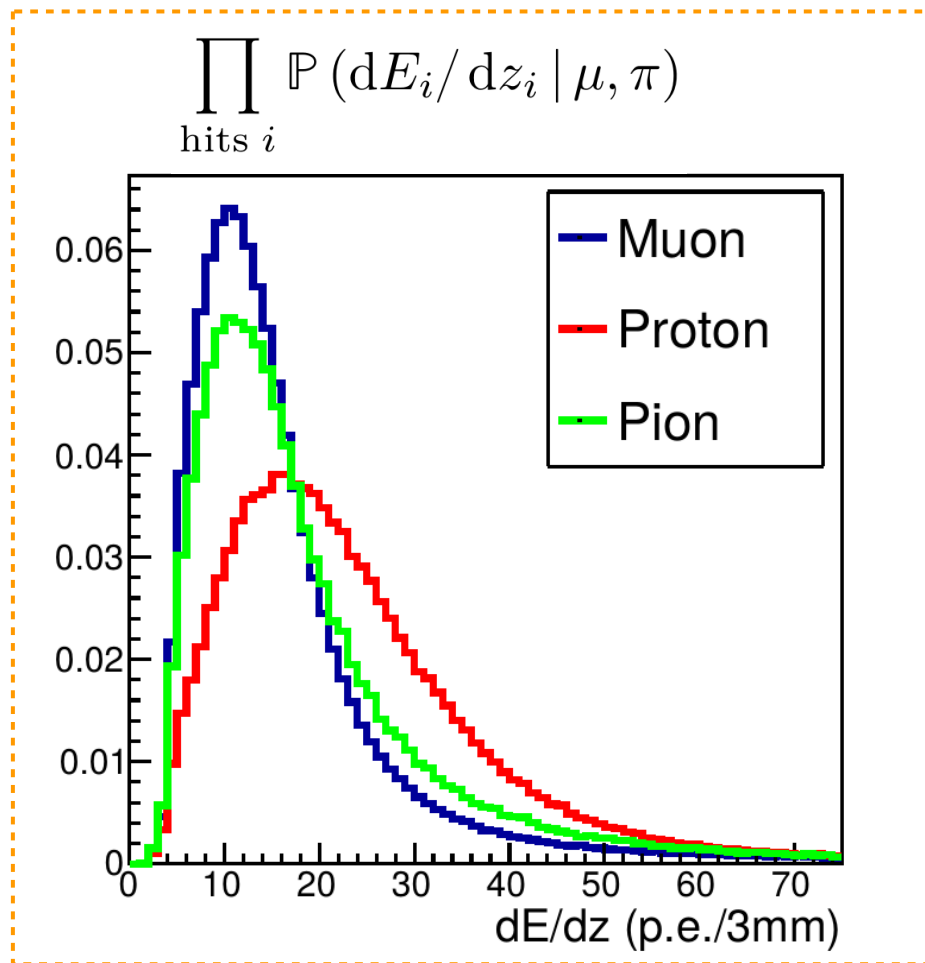
	$p_\mu$ range/ resolution	$\theta_\mu$ range/ resolution
Through-going $\mu$	$> 1 \text{ GeV}/c$	$0 - 50^\circ / 5^\circ$
Stopping $\mu$	$0.4 - 1 / 0.1 \text{ GeV} / c$	$0 - 50^\circ / 5^\circ$

# CC1 $\pi$ selection tool

6

- Based on a PID to avoid cross-section model dependency.

$\mu, \pi$ -likelihood:  $\mathbb{P}(\mu, \pi | \{dE/dz\}) = \frac{\mathbb{P}(\{dE/dz\} | \mu, \pi) \mathbb{P}(\mu, \pi)}{\mathbb{P}(\{dE/dz\})}$



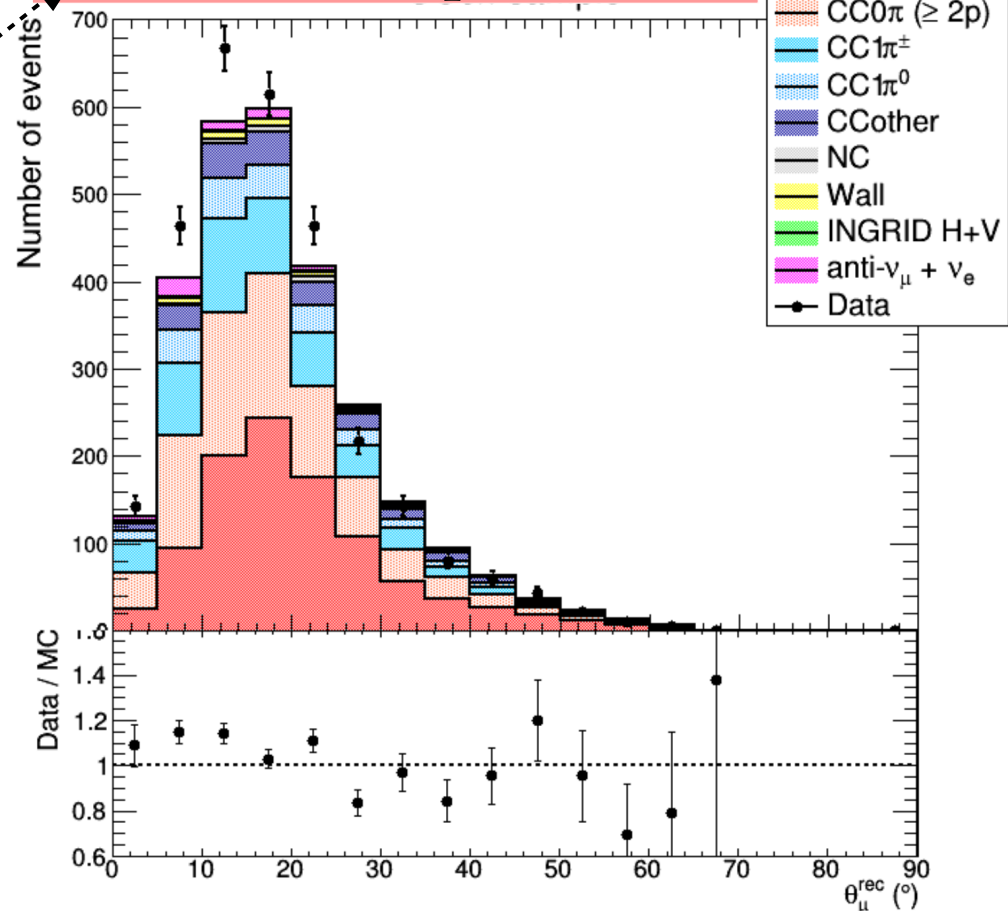
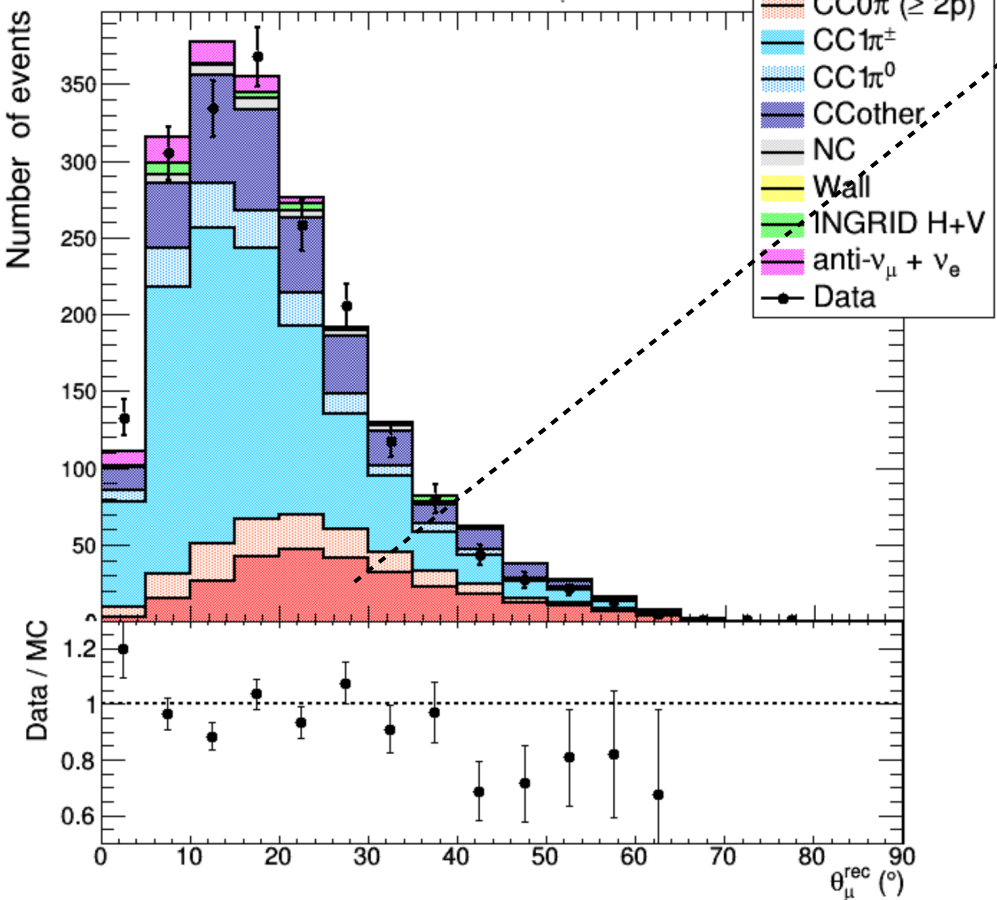
# CC1 $\pi$ and CC0 $\pi$ selection results

**CC 1 $\pi$**  :  $\nu_\mu + \mathcal{N} \rightarrow \mu^- + \pi^\pm + \mathcal{N}'$

**CC 0 $\pi$**  :  $\nu_\mu + \mathcal{N} \rightarrow \mu^- + \mathcal{N}'$

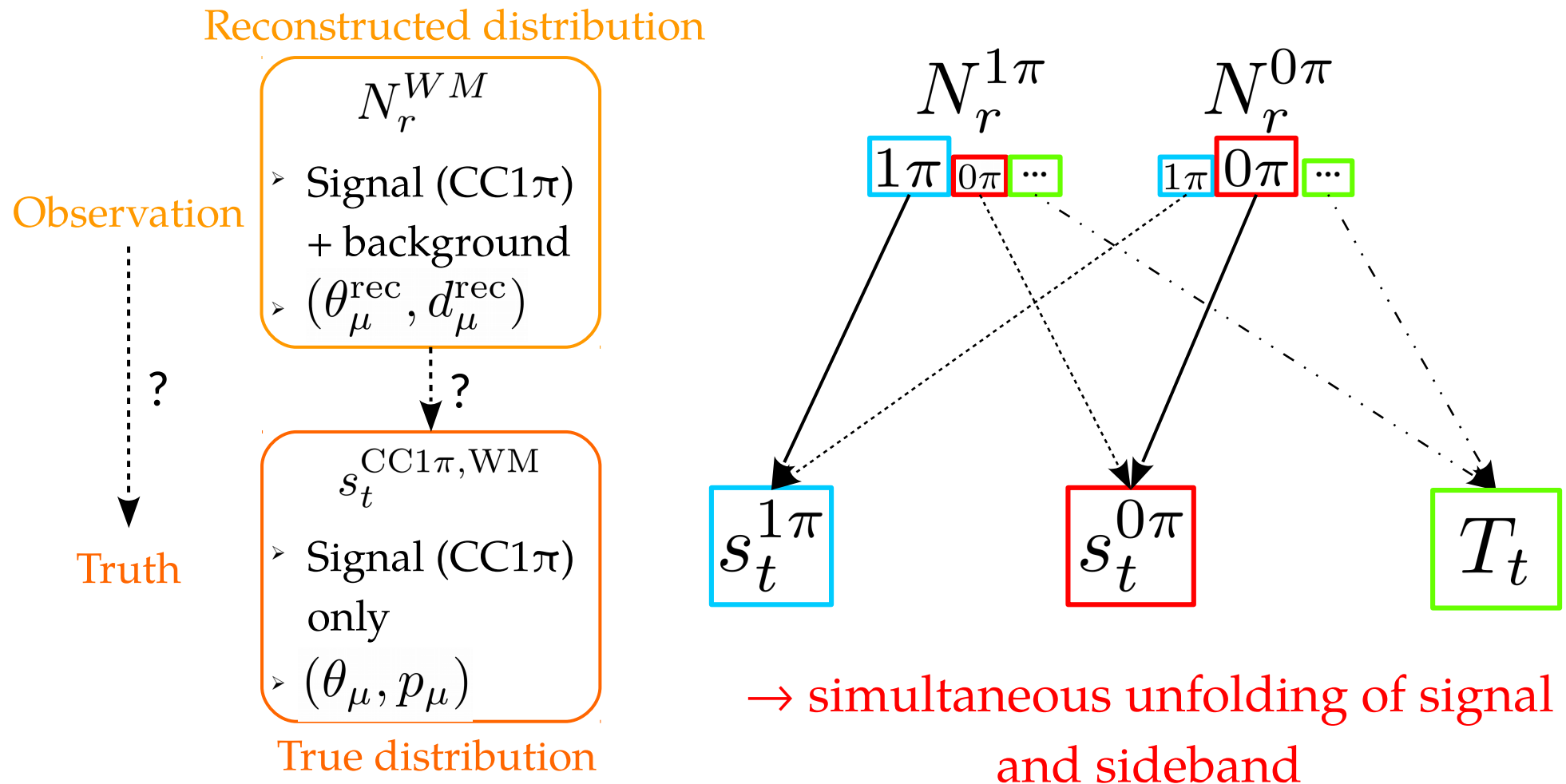
**Signal** : 2 tracks  $\mu$ -like  
(+ 0 or 1 track p-like)

**Side-band** : 1 track  $\mu$ -like  
+ 1 track p-like



# Unsmearing the detector effects

Goal: model independent result in observable variables  $(\theta_\mu, p_\mu)$   
→ For everyone external to collaboration to use





# Bayes inspired unfolding

Unsmearing done with a Bayes inspired unfolding matrix

Input Data

$$U_i^j \equiv P(T_i|O_j) = \frac{P(O_j|T_i) \cdot P(T_i)}{\sum_k P(O_j|T_k) \cdot P(T_k)}$$

Likelihood  
= Detector transfer  
matrix

Prior on  $p_\mu, \theta_\mu$  of CC1 $\pi$  events  
(NEUT etc.)  $\rightarrow$  Model dependency

$$D^{(1) \text{ true},i} = \sum_j U_j^i \times D^j$$

# Iterative procedure

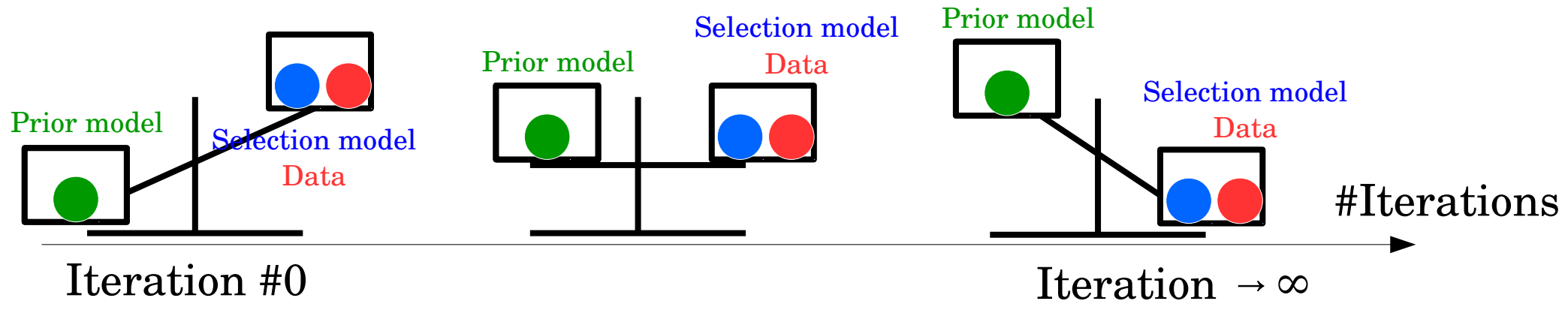
Unsmearing done with a Bayes inspired unfolding matrix

Input Data

$$U_i^j \equiv P(T_i|O_j) = \frac{P(O_j|T_i) \cdot P(T_i)}{\sum_k P(O_j|T_k) \cdot P(T_k)}$$

$$D^{(1) \text{ true},i} = \sum_j U_j^i \times D^j$$

$$U_i^{j(2)} = \frac{P(O_j|T_i) \cdot D^{(1) \text{ true},i}}{\sum_k P(O_j|T_k) \cdot D^{(1) \text{ true},k}}$$



How to choose  $N_{\text{iterations}}$  ?

# Unsmearing the detector results

Goal : convergence towards the true value. For fake data/MC :

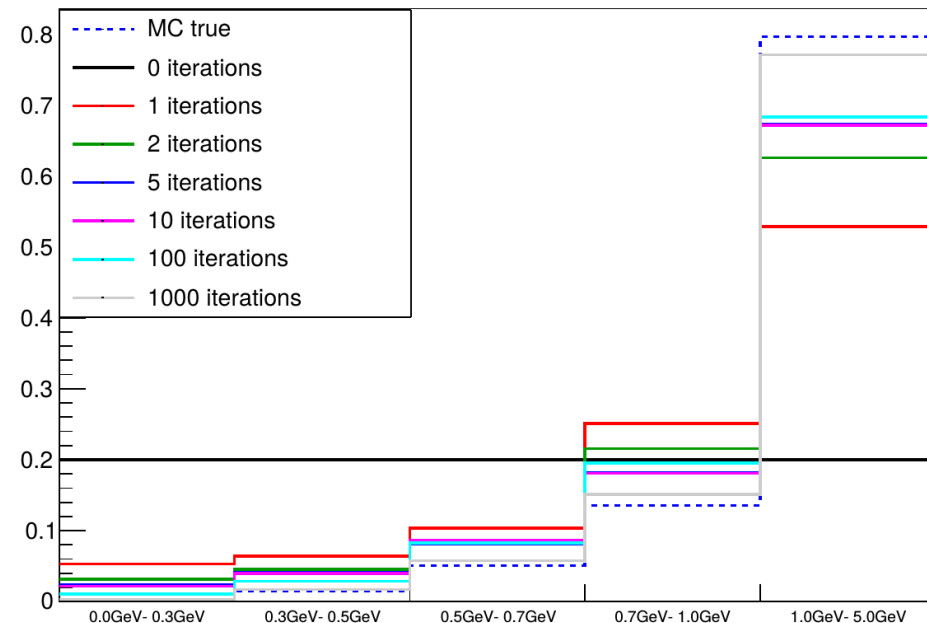
$$\chi_T^2 = \sum_{\text{true } p_i, \text{true } \theta_j} \sum_{\text{true } p_k, \text{true } \theta_l} (N_{i,j}^{\text{Unfolded}, It a} - N_{i,j}^{\text{True}}) \cdot (V^{-1})_{k,l}^{i,j} \cdot (N_{k,l}^{\text{Unfolded}, It a} - N_{k,l}^{\text{True}})$$

Wish : bias  $\ll$  total uncertainty  $\implies \frac{1}{N_{bins}} \chi_T^2 < 0.2$       Bias  $\leq 10\%$  Uncertainty

Data : impossible to evaluate "true value" .

Solution #1 : Define convergence point  
with simulation / mock data

- Model dependency  $\rightarrow$  may not be optimal for data if  $\neq$  model.
- $N_{it}$  too small: under-estimate bias.
- too big: over-estimate stat. uncertainty



# Data driven convergence criterion

12

Solution #2 : Convergence towards data final value,  $N^\infty$  (data-driven)

$$\chi_{DD}^2 = \sum_{\text{true } p_i, \text{true } \theta_j} \sum_{\text{true } p_k, \text{true } \theta_l} (N_{i,j}^{\text{Unfolded}, It^a} - N_{i,j}^{\text{Unfolded}, It^\infty}) \cdot (V^{l-1})_{k,l}^{i,j} \cdot (N_{k,l}^{\text{Unfolded}, It^a} - N_{k,l}^{\text{Unfolded}, It^\infty})$$

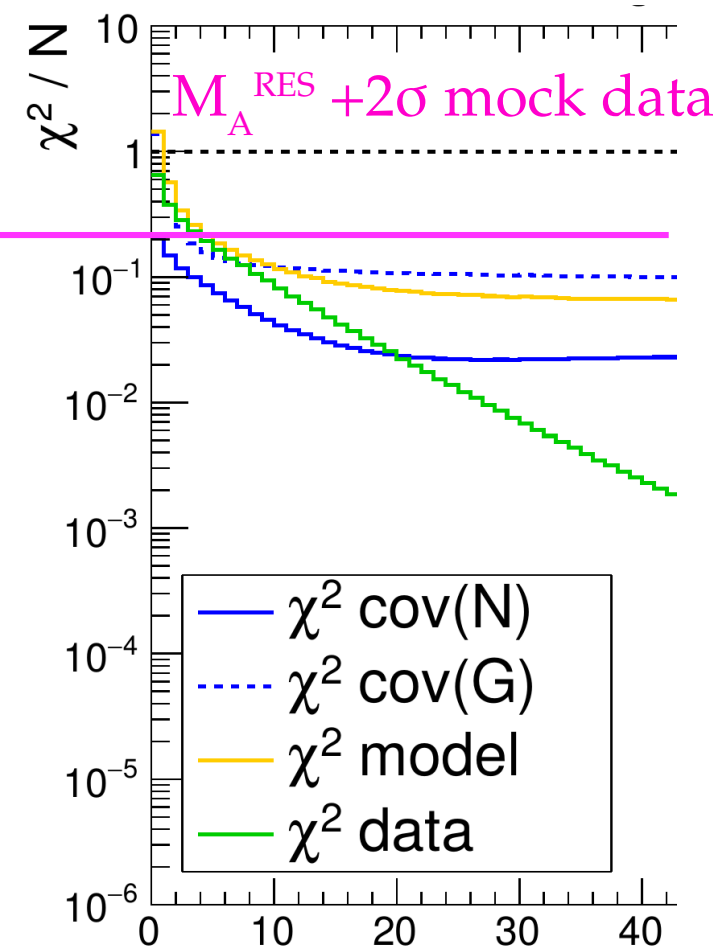
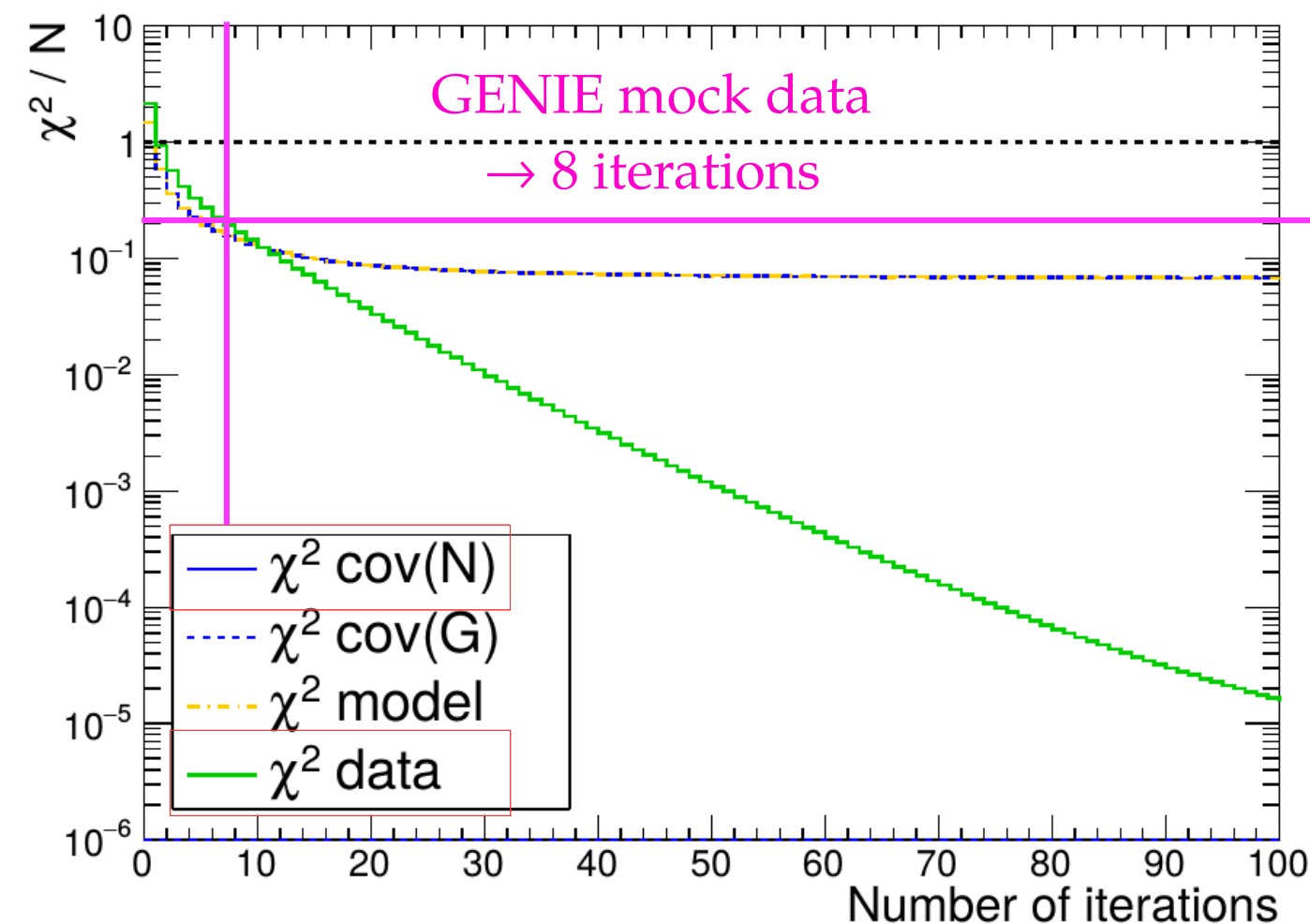
• Analytically : convergence to  $N^\infty \Rightarrow$  convergence to  $N^{\text{True}}$

• Use fake data sets to show that  $\frac{1}{N_{bins}} \chi_{DD}^2 < \boxed{0.25} \implies \frac{1}{N_{bins}} \chi_T^2 < \boxed{0.2}$

➤ PM: 11 iterations and WM: 16 iterations

# Mock-data

13



1.  $N_{\text{it}}^{\text{data}} \gg N_{\text{it}}^{\text{mock data studies}} (\leq 8)$

2. Most mock-data converge for 1 iteration ...

→ See S. Dolan talk on unfolding

→ Do not trust MC  
for unfolding !

→ Essential to use  
data-driven criterion ?

# Detector cross sections

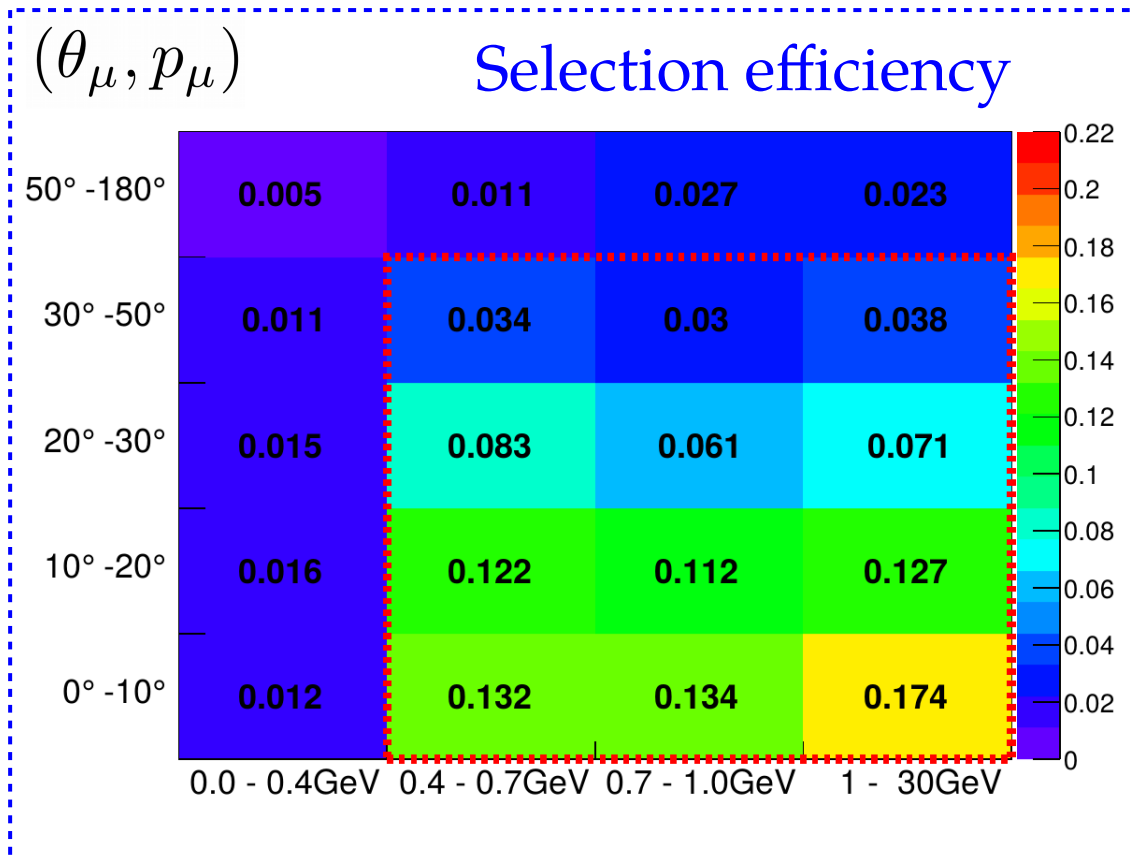
CC1 $\pi$  cross section in a given detector :

$$\frac{d^2\sigma_t^{\text{CC1}\pi}}{d\theta_\mu dp_\mu} \equiv \frac{1}{\Delta\theta_\mu \Delta p_\mu} \cdot \frac{s_t^{\text{CC1}\pi}}{e_t \times \Phi \times T}$$

Number of CC1 $\pi$  events (from unfolding)

Neutrino flux

Target nucleons



Accessible phase space:

$$\theta_\mu < 50^\circ, \quad p_\mu > 400 \text{ MeV}$$

# Uncertainties

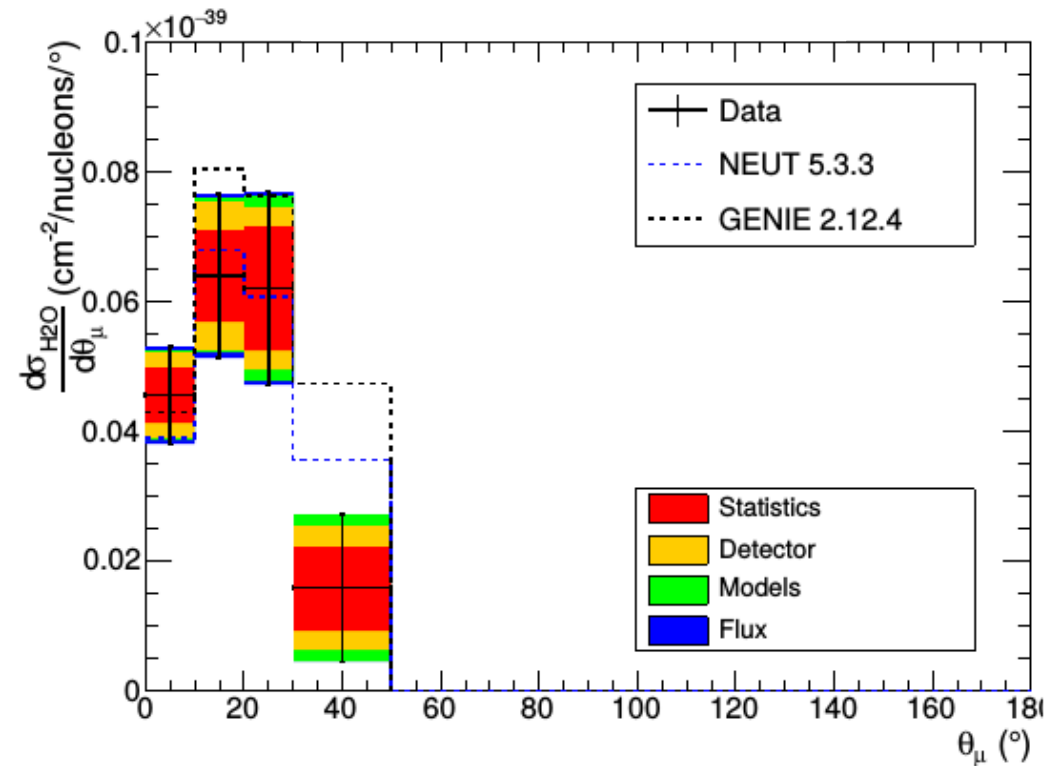
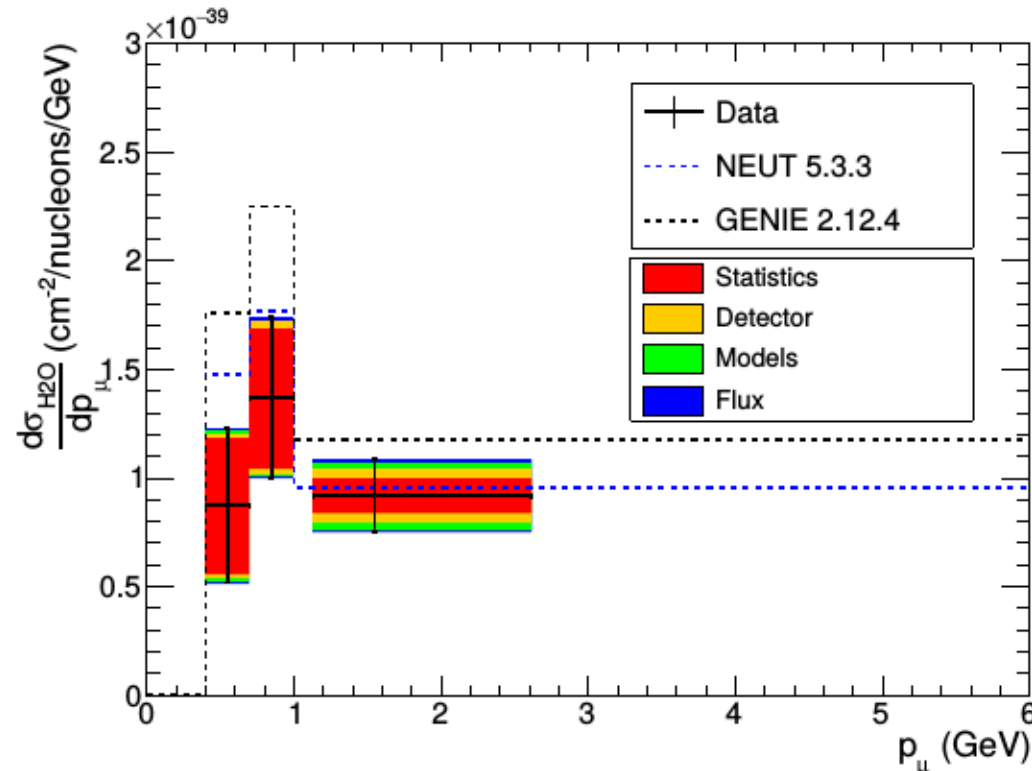
Systematic source	$\Delta\sigma_{\text{CH}}(\%)$	$\Delta\sigma_{\text{H}_2\text{O}}(\%)$	$\Delta\sigma_{\text{H}_2\text{O}}/\sigma_{\text{CH}}(\%)$
Statistics	4.8	8.7	10.8
Flux	6.6	6.8	1.1
Model	7.5	7.6	6.9
Detector	7.9	6.6	9.9
Systematics	12.7	12.1	12.1
Total	13.6	14.9	16.2

Summary of the all uncertainties on the 1-bin cross sections.

# Differential result and model comparison

16

Single differential cross section on water :



	CH-only	H <sub>2</sub> O-only	CH+H <sub>2</sub> O
$\chi^2(\text{Data} \mid \text{NEUT})/\text{NDF}$	2.0 (2.3 $\sigma$ )	1.3 (1.2 $\sigma$ )	1.3 (1.4 $\sigma$ )
$\chi^2(\text{Data} \mid \text{GENIE})/\text{NDF}$	3.7 (4.3 $\sigma$ )	2.6 (3.1 $\sigma$ )	2.4 (3.7 $\sigma$ )

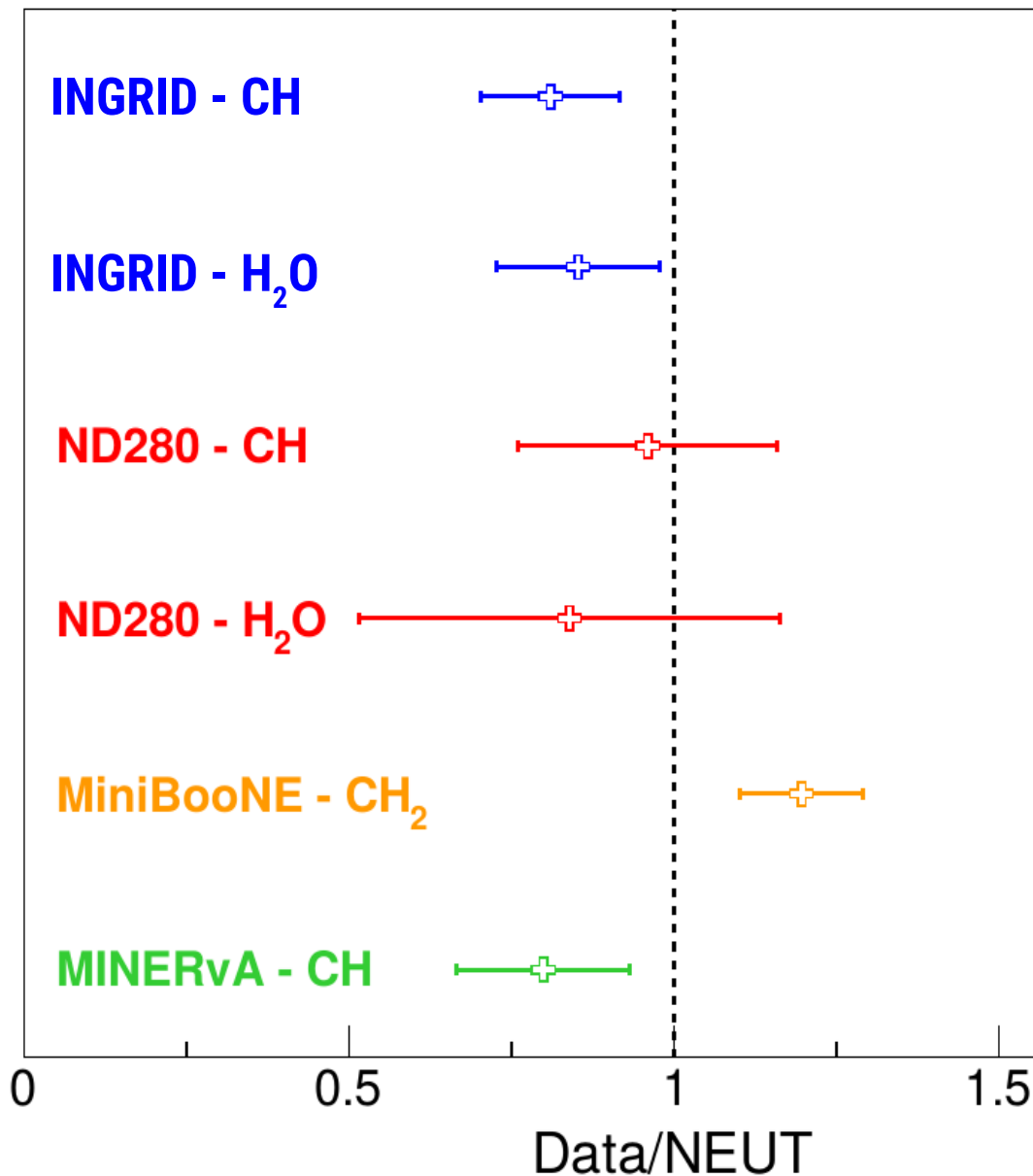
- Our measurement is below NEUT and GENIE.
- NEUT still provides best agreement → High momentum bin



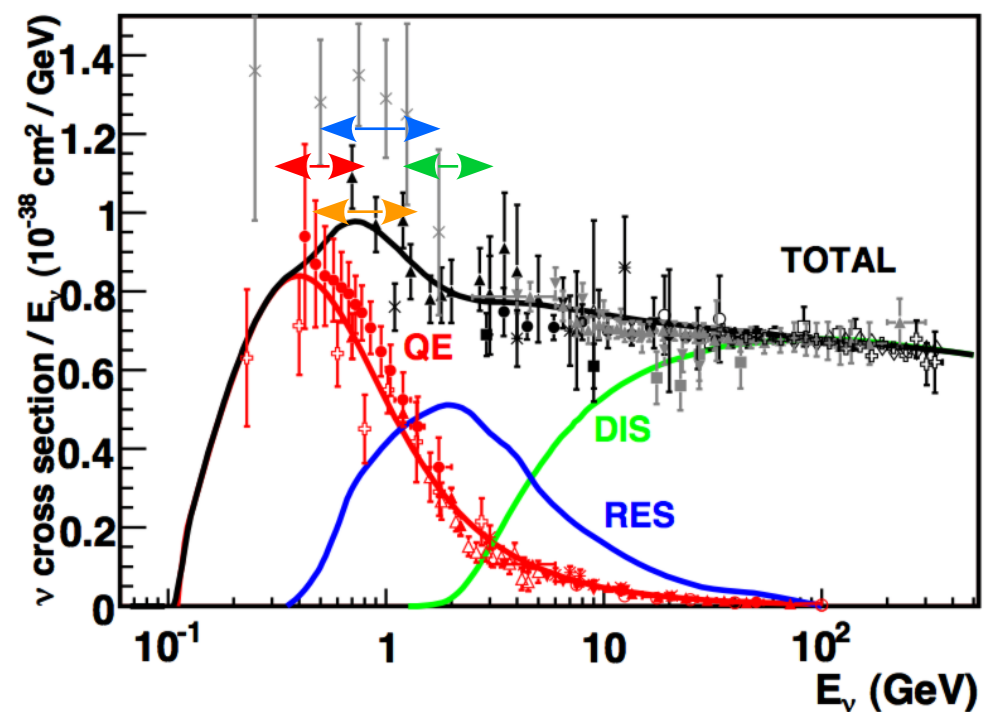
# Comparison with other results

17

## CC1 $\pi$ cross sections

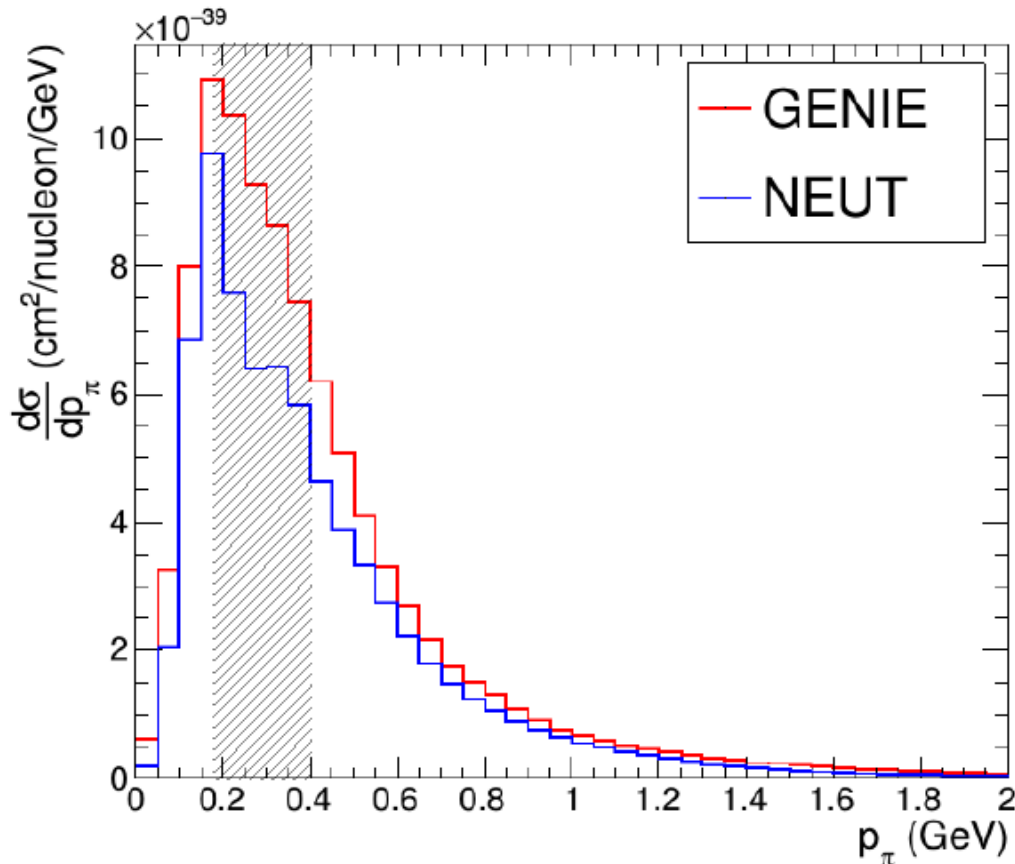


- Compatible w/ all other results (< NEUT) but MiniBooNE.
- Most accurate result on H<sub>2</sub>O



# NEUT and GENIE final state interactions

18



Incomplete intra-nucleus cascade

Complete intra-nucleus cascade

Intra-nuclear cascade

Interaction w/  
free nucleons  
 $\pi^+ n \rightarrow \pi^+ n$

Nuclear model  
 $\rho(\mathbf{r})$

Higher suppression of  $\pi$  in NEUT

If  $\pi$  absorption is higher in data  $\rightarrow$  should see an increase in  $CC0\pi$ .

Will be refined with a  $CC0\pi$  /  $CC1\pi$  join fit : coming this year.

# Conclusions

19

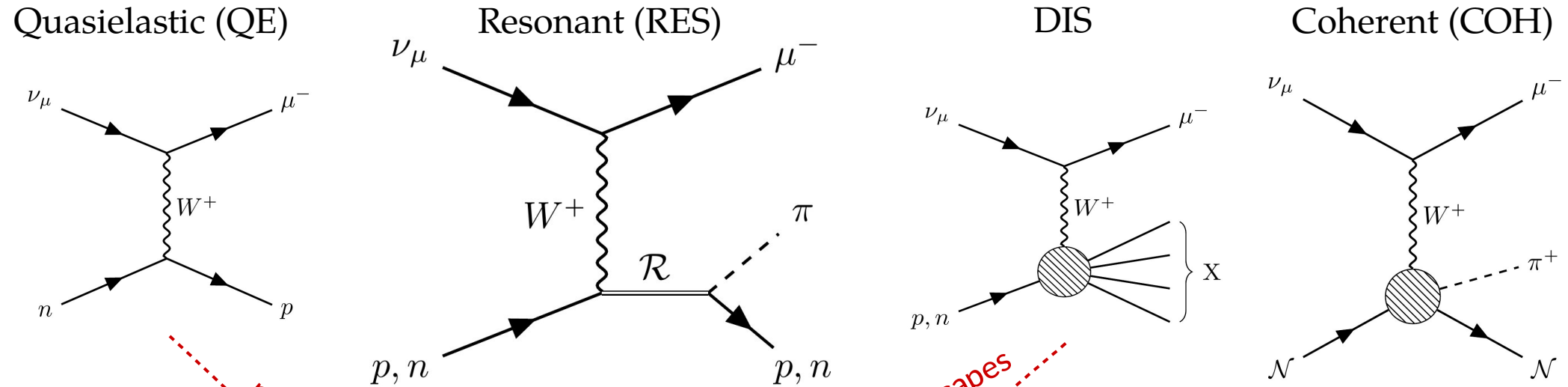
- High uncertainties on  $CC1\pi$  cross-section  $\rightarrow$  impact oscillations  
 $\rightarrow$  Produce a more accurate measurement of  $CC1\pi$  cross-section on  $H_2O$
- Developed a data-driven unfolding method for the first time to reduce model-dependency.

## Take home message :

- Not using data-driven unfolding  $\rightarrow$  model bias.
  - Our  $CC1\pi$  data shows a deficit  $\rightarrow$  as Minerva and ND280 results.
  - Which agrees considerably better with NEUT than GENIE.
- To investigate its cause properly  
 $\rightarrow$  Is available and will be published for experts (=theorists) to use.  
 $\rightarrow$  Need a  $CC0\pi/CC1\pi$  join fit  $\rightarrow$  coming this year.

# Additional slides

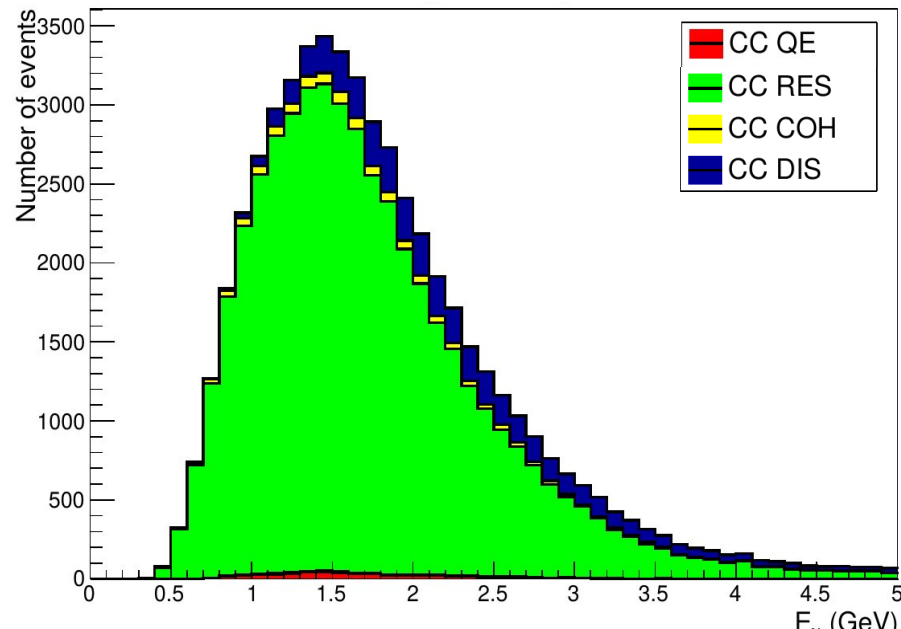
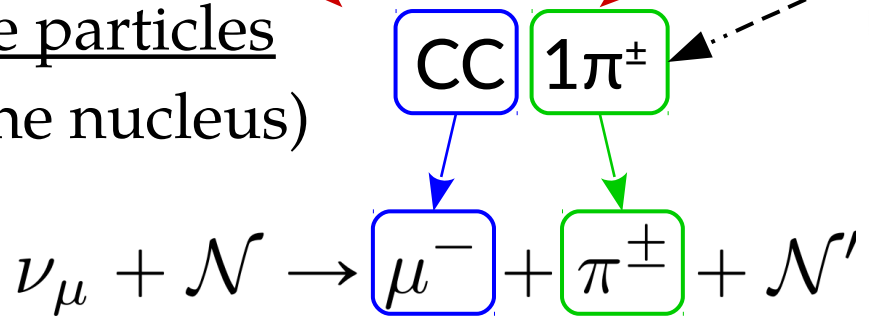
# CC1 $\pi$ signal definition



*production of a  $\pi$*

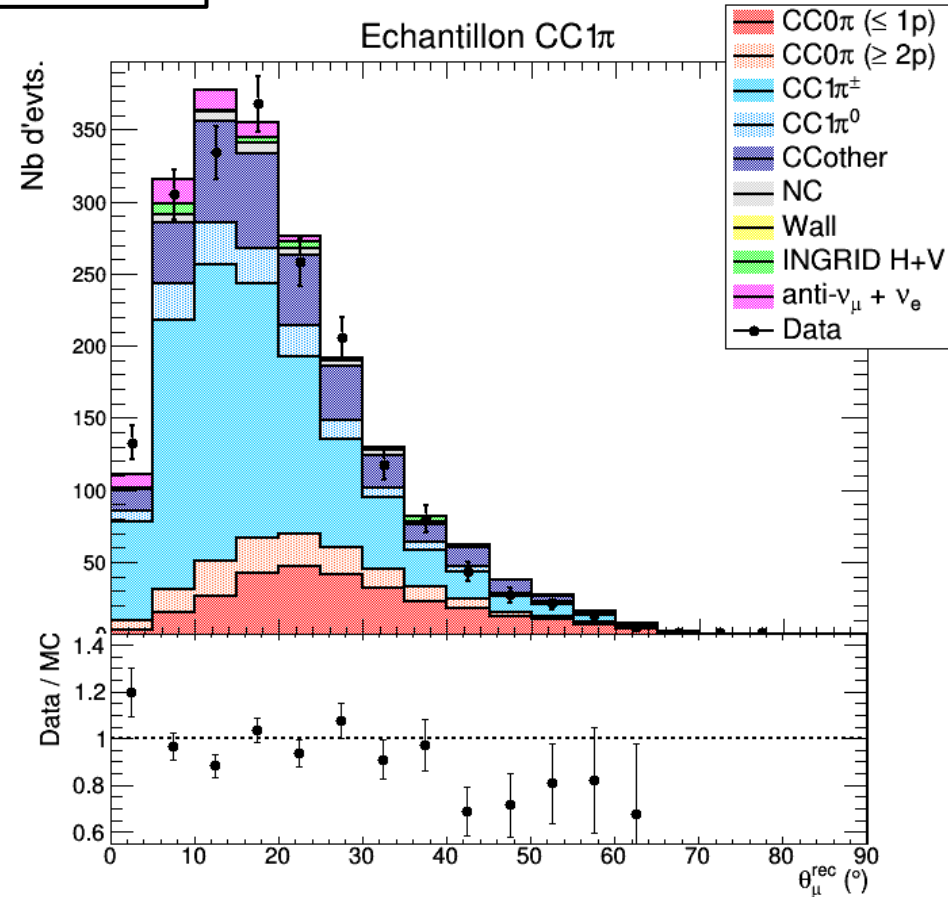
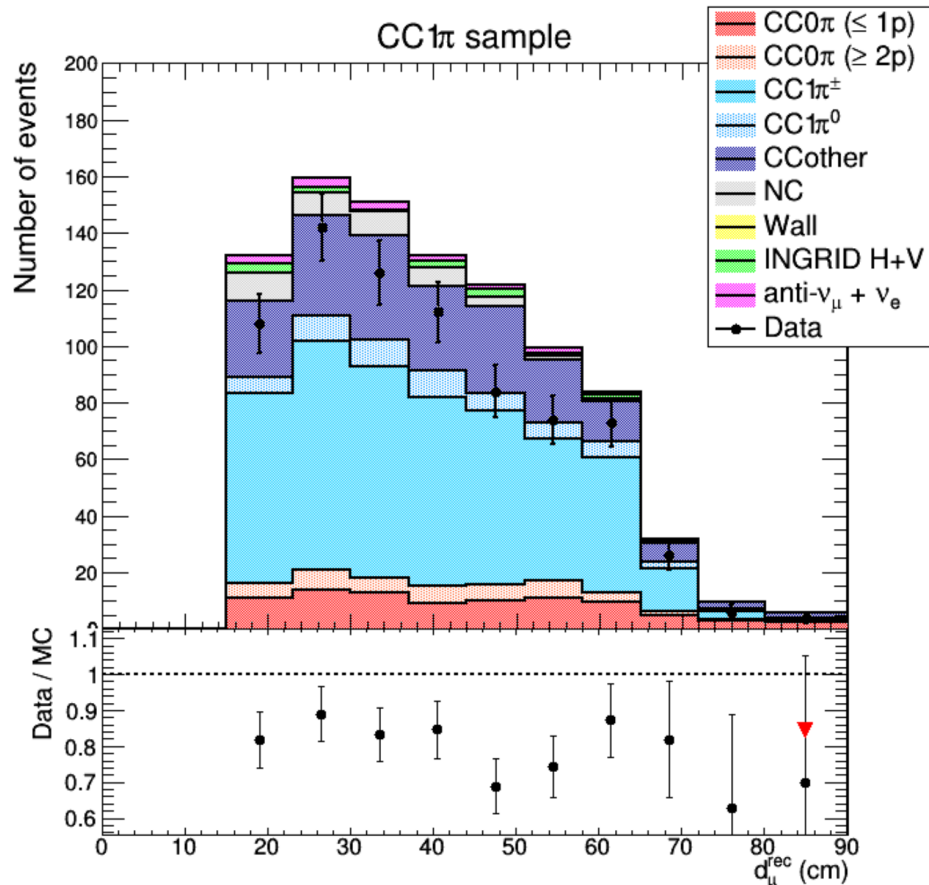
*Only a  $\pi$  escapes the nucleus*

Observable particles  
(escaping the nucleus)



# CC1 $\pi$ -selected sample, the signal

2 tracks  $\mu$ -like  
(+0 or 1 track p-like)



Cut	Data	Total MC	CC0 $\pi$	CC1 $\pi^{\pm}$	CC1 $\pi^0$	CCOther	NC	Ext.	$\bar{\nu}_{\mu} + \nu_e$
CC inclusive	34689	34363	14144	7764	2444	5836	1253	1663	1259
CC1 $\pi$ (PID)	4090	5437	994	2454	319	1377	116	31	146
2 or 3 tracks	3513	5016	989	2376	302	1088	100	30	133
$\mu$ stop/through	2344	2812	502	1416	166	582	44	14	87

↖ Main contamination → Side band

# Cross-section model systematic uncertainties

## W/o side-band

## W/ side-band

Parameter	$\Delta\sigma_{\text{CH}}(\%)$	$\Delta\sigma_{\text{H}_2\text{O}}(\%)$	$\Delta\sigma_{\text{H}_2\text{O}}/\sigma_{\text{CH}}(\%)$	Parameter	$\Delta\sigma_{\text{CH}}(\%)$	$\Delta\sigma_{\text{H}_2\text{O}}(\%)$	$\Delta\sigma_{\text{H}_2\text{O}}/\sigma_{\text{CH}}(\%)$
$p_F$ $^{12}\text{C}$	0.13	0.02	0.11	$p_F$ $^{12}\text{C}$	< 0.1	< 0.1	< 0.1
$p_F$ $^{16}\text{O}$	-	0.20	0.20	$p_F$ $^{16}\text{O}$	-	0.2	0.2
$E_B$ $^{12}\text{C}$	0.01	< 0.01	0.01	$E_B$ $^{12}\text{C}$	< 0.1	< 0.1	< 0.1
$E_B$ $^{16}\text{O}$	-	0.01	0.01	$E_B$ $^{16}\text{O}$	-	< 0.1	< 0.1
MEC norm $^{12}\text{C}$	4.60	0.08	4.56	MEC norm $^{12}\text{C}$	2.1	0.8	2.5
MEC norm $^{16}\text{O}$	-	4.80	4.80	MEC norm $^{16}\text{O}$	-	3.7	3.7
$M_A^{QE}$	8.62	13.60	4.81	$M_A^{QE}$	2.8	5.1	2.1
$C_A^5$	1.01	2.07	1.06	$C_A^5$	3.8	2.7	1.1
$M_A^{RES}$	2.75	4.22	1.46	$M_A^{RES}$	3.2	1.1	1.9
$I = 1/2$ Bkg	2.17	3.19	1.09	$I = 1/2$ Bkg	0.3	1.3	0.8
CC-other shape	5.91	4.81	1.11	CC-other shape	3.1	0.8	1.7
CC-coherent norm $^{12}\text{C}$	0.82	0.01	0.81	CC-coherent norm $^{12}\text{C}$	0.4	< 0.1	0.4
CC-coherent norm $^{12}\text{O}$	-	0.81	0.81	CC-coherent norm $^{12}\text{O}$	-	0.3	0.3
NC-coherent norm	< 0.01	< 0.01	< 0.01	NC-coherent norm	< 0.01	< 0.1	< 0.1
NC-other shape	0.59	0.81	0.23	NC-other shape	0.1	0.3	0.3
FSI $\pi$ absorption	1.05	0.25	0.88	FSI $\pi$ absorption	0.8	1.7	2.4
FSI charge exchange, LE	0.61	0.42	0.19	FSI charge exchange, LE	0.8	0.2	1.0
FSI charge exchange, HE	0.32	0.33	0.01	FSI charge exchange, HE	0.2	0.9	0.7
FSI $\pi$ QE scattering, LE	2.75	1.28	1.57	FSI $\pi$ QE scattering, LE	2.6	0.4	2.8
FSI $\pi$ QE scattering, HE	0.76	1.28	0.54	FSI $\pi$ QE scattering, HE	0.8	1.0	0.2
FSI $\pi$ production	0.53	0.90	0.37	FSI $\pi$ production	0.5	0.8	0.2
Total	12.4	16.4	8.8	Total	7.5	7.6	6.9

# Detector systematic uncertainty

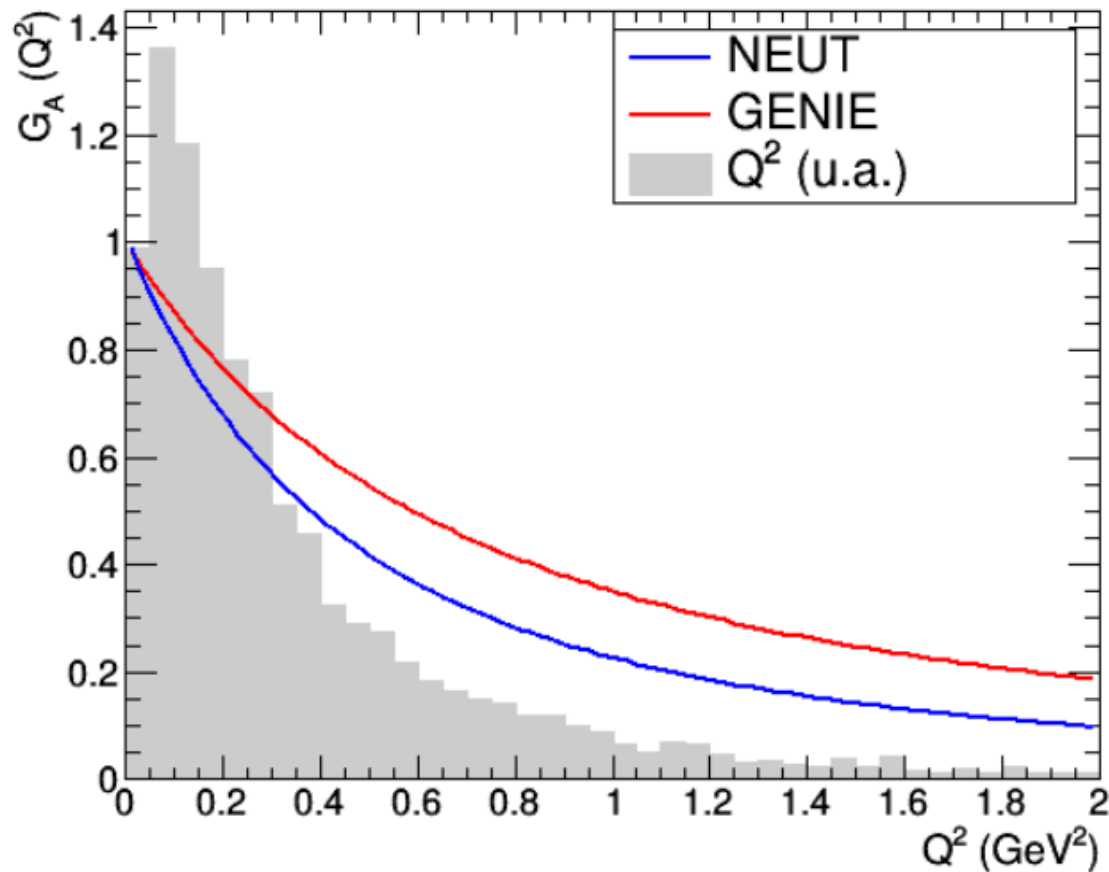
18

Systematic source	$\Delta\sigma_{\text{CH}}(\%)$	$\Delta\sigma_{\text{H}_2\text{O}}(\%)$	$\Delta\sigma_{\text{H}_2\text{O}}/\sigma_{\text{CH}}(\%)$
Hit Efficiency	0.1	1.2	1.2
Light yield vs. angle	7.2	4.3	9.0
Birks saturation*	2.3	3.2	1.6
External backgrounds*: Wall	1.2	1.4	0.1
INGRID	0.1	0.1	0.1
Secondary interactions	1.1	1.5	2.0
Cross-talk	-	0.7	0.7
Reconstruction	1.3	1.6	2.3
Event pile-up	0.5	0.6	0.8
Target mass	0.4	0.3	0.5
Total	7.9	6.6	9.9



# NEUT and GENIE form factors

15



$$G_A^{\text{GS}}(Q^2) = C_A^5(0) \left( 1 + \frac{Q^2}{(M_A^{\text{RES}})^2} \right)^{-2}$$

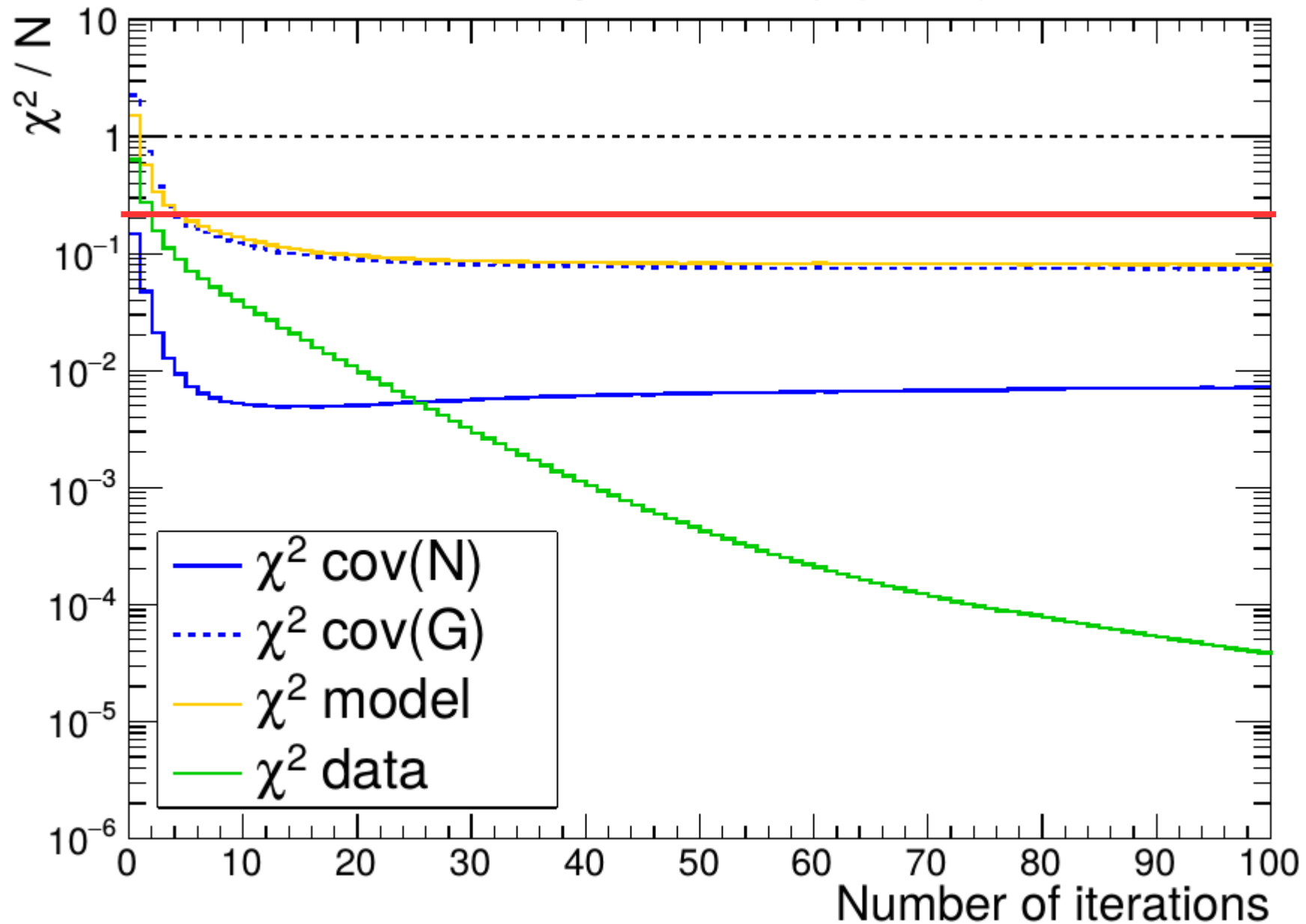
$$C_A^5(0) = 1.01, \quad M_A^{\text{RES}} = 0.95 \text{ GeV}/c^2$$

$$G_A^{\text{RS}}(Q^2) = \left( 1 + \frac{Q^2}{4m_N^2} \right)^{1/2-n} \left( 1 + \frac{Q^2}{(M_A^{\text{RES}})^2} \right)^{-2}$$

$$M_A^{\text{RES}} = 1.12 \text{ GeV}/c^2$$

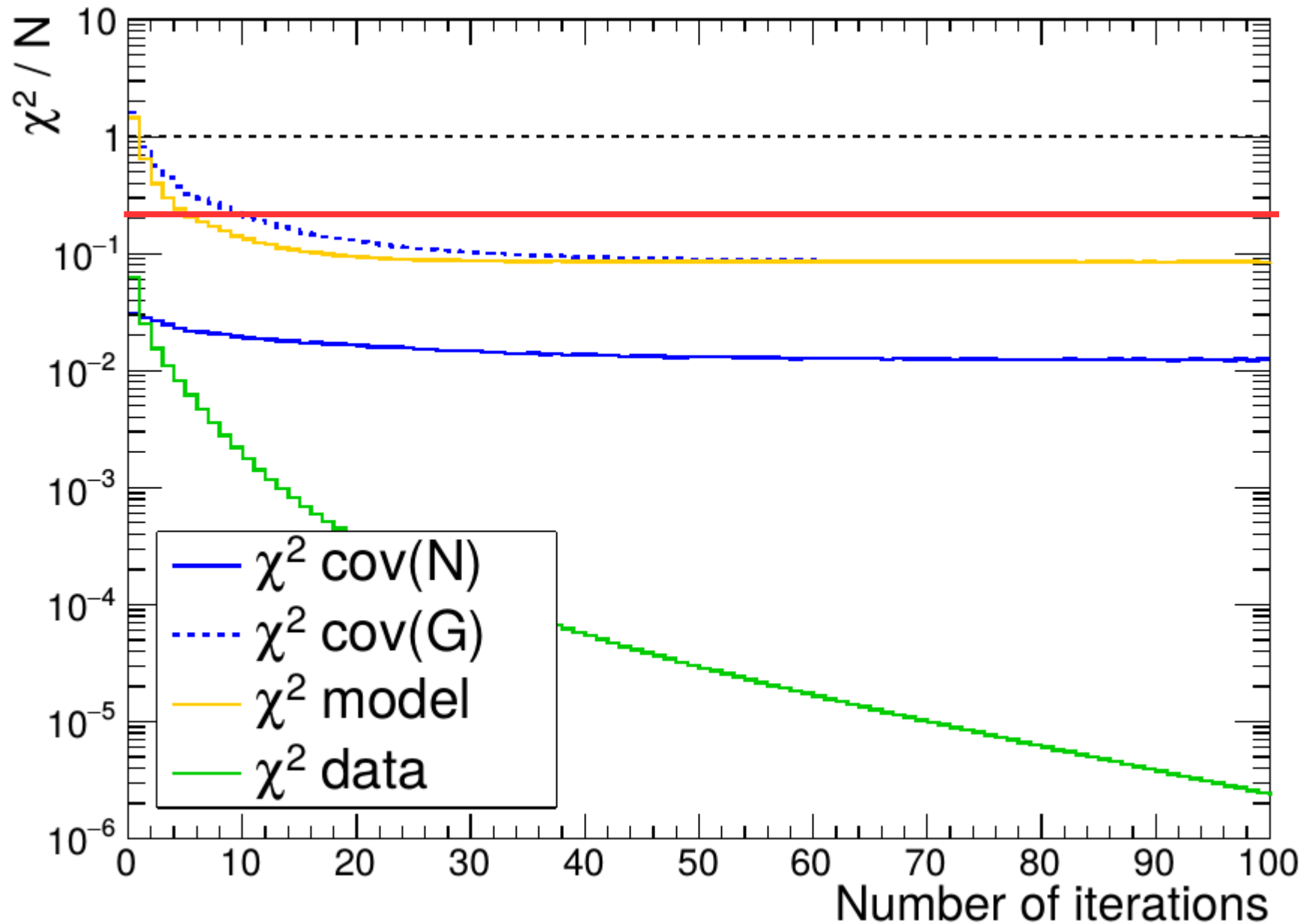
# CC-Coherent-varied mock data

23



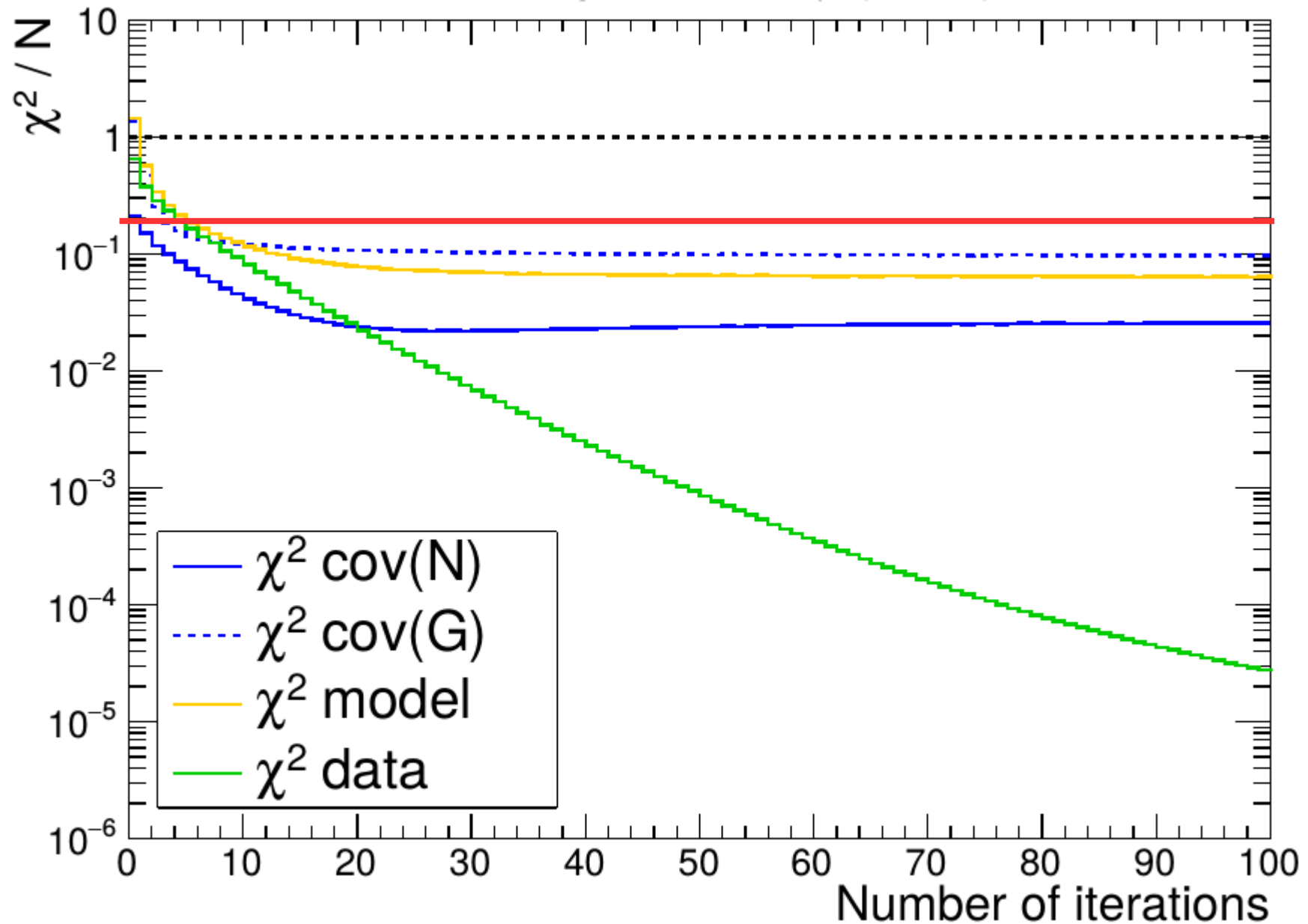
# MAQE-varied mock data

23



# MARES-varied fake data

23



# GENIE-varied fake data

23

